Mineralogical Magazine, February 1998, Vol. 62(1), pp. 65–75

A single crystal, linearly polarized Fe 2*p* X-ray absorption study of gillespite

P. F. SCHOFIELD[1], G. VAN DER LAAN[2], C. M. B. HENDERSON[2,3] AND G. CRESSEY[1]

[1] Department of Mineralogy, Natural History Museum, Cromwell Road, London SW7 5BD, UK
[2] Synchrotron Radiation Department, Daresbury Laboratory, Warrington WA4 4AD, UK
[3] Department of Earth Science, University of Manchester, Manchester M13 9PL, UK

ABSTRACT

The Fe 2*p* X-ray absorption spectra of single crystal gillespite, $BaFeSi_4O_{10}$, show a strong linear dichroism, i.e. a large difference in the absorption when measured with the polarization of the X-rays either parallel or perpendicular to the plane of the FeO_4 group. The isotropic spectrum, obtained from measurement at the 'magic angle', and the polarization dependent spectra have been compared to atomic multiplet calculations and show an excellent agreement with theory. Analysis of the branching ratio, the linear dichroism, and the detailed peak structure confirms that the $^5A_1$ level is the ground state at room temperature and pressure. The $^5B_2$ level is sufficiently low in energy that a distortion of the electronic charge density, induced by increased pressure, may result in a $^5B_2$ ground state.

KEYWORDS: gillespite, X-ray absorption spectroscopy, linear dichroism.

Introduction

GILLESPITE ($BaFe^{2+}Si_4O_{10}$), first described by Schaller (1922), is a rare, naturally-occurring sheet silicate, unusual in that Fe^{2+} is present in square-planar coordination with oxygen ligands. At room temperature and pressure gillespite is tetragonal, space group *P*4/*ncc* (Pabst, 1943; Wainright, 1969; Hazen and Burnham, 1974). The silicate layers are formed by 4-membered rings of SiO_4 tetrahedral units, with each ring connected to four other inverted 4-membered rings of SiO_4 tetrahedral units via the apical oxygens (Fig. 1). The two layers of 4-membered rings making up the Si_8O_{20} double layers are rotated by approximately 15° relative to each other, hence, the *c* cell parameter spans two silicate layers. These layers are linked by Ba atoms that occupy eight-coordinate sites at the Wyckoff position *b* (0,0,0). In each silicate layer the Fe^{2+} cations, located at Wyckoff position *c* (0, 0.5, *z*), are bonded to oxygens of 4 separate silicate rings in a square planar arrangement in which the oxygen ligands are not quite co-planar. These Fe sites are above (or below) the centres of the 4-membered SiO_4 rings of the adjoining silicate layer (Fig. 1).

Gillespite undergoes an unusual and complicated pressure-induced structural phase transition (Strens, 1966; Hazen and Burnham, 1974; Hazen and Finger, 1983; Redfern *et al.*, 1993; Henderson *et al.*, 1995) in which the tetragonal *P*4/*ncc* structure (gillespite I) changes to an orthorhombic $P2_12_12_1$ structure (gillespite II). This phenomenon is accompanied by a startling colour change from red to blue. Strens (1966) first observed this phase transition by optical absorption spectroscopy and attributed the colour change to a modification of the electronic structure of Fe^{2+} from high- to low-spin. Abu-Eid *et al.* (1973) subsequently interpreted polarized optical absorption spectra to suggest that it was due to the square-planar Fe^{2+} coordination becoming distorted in the high-pressure phase. High-pressure Mossbauer spectroscopy of a synthetic gillespite sample was used to confirm the latter interpretation (Huggins *et al.*, 1975; 1976). Huggins *et al.* (1975) also reported the presence of a second Fe^{2+} site in the high-pressure phase (11% of the total Fe^{2+} sites) but commented that a similar, weaker doublet also

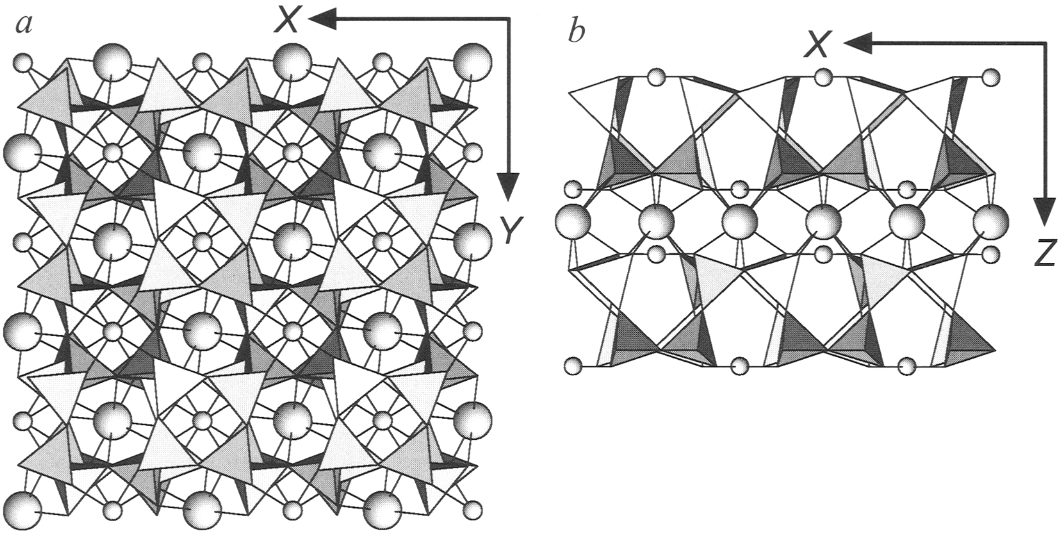

FIG. 1. The crystal structure of gillespite with a view onto the *xy*-plane (*a*) and the *xz*-plane (*b*). Large open circles represent the Ba atoms, small shaded circles Fe, and polyhedra the SiO_4 tetrahedra.

occurred in the 1 bar Mossbauer spectrum. Huggins *et al.* (1976) subsequently suggested that this second Fe^{2+} site may become dominant in a still-higher-pressure phase occurring at above 70 kbar.

Hazen and Finger (1983) revised earlier structural work on the gillespite phases and suggested that the phase transition occurs when the Ba polyhedron collapses from a distorted cubic coordination to a 10-coordinated geometry. These changes are accompanied by the *trans* O—Fe—O bond angles of the essentially square-planar Fe site decreasing from 178.5° at 1 bar to 157° at 21 kbar, resulting in the Fe-site adopting the geometry of a flattened tetrahedron (cf. an ideal tetrahedral angle of 109.5°). Hazen and Finger (1983) thus associated the colour change with changes in the crystal-field resulting from distortion of the Fe^{2+} site. They also concluded that there was no evidence for the 70 kbar phase transition and suggested that the second Mossbauer doublet in the synthetic gillespite used by Huggins *et al.* (1976) could be due to 'a few percent Fe^{2+}' entering the Ba site.

Mackey *et al.* (1979) measured the single-crystal magnetic anisotropy of gillespite from 4.2 to 298 K. They obtained good agreement between calculated and observed magnetic susceptibility parameters using a crystal-field model assuming a $^5A_{1g}$ ground state, and with excited state energies compatible with the electronic spectrum observed by optical absorption spectroscopy. They used their model to calculate the dependence of the *d–d* transition energies on varying the *trans*-O—Fe—O angle and used the optical absorption data of Abu-Eid *et al.* (1973) to predict a value of about 150.5° for the O—Fe—O angle in gillespite-II (i.e. only slightly lower than that determined by Hazen and Finger (1983) at 21 kbar).

2*p* X-ray absorption spectroscopy

2*p* X-ray absorption spectroscopy (XAS) is a sensitive probe for the electronic structure of 3*d* transition metal ions with a specificity for element, site-symmetry and valency (van der Laan and Kirkman, 1992). The advent of dedicated beamlines for the soft X-ray region using high-energy gratings to monochromatize synchrotron radiation has enabled access across the entire 3*d* transition metal series. Cressey *et al.* (1993) detailed the applicability of 2*p* XAS to the problems encountered in chemically complex minerals, such as multiple valence states. Other applications such as the identification of high- and low-spin states (van der Laan *et al.*, 1988), oxidation state identification and valence ratio quantification (Cressey *et al.*, 1993; Henderson *et* *al.*, 1995; Schofield *et al.*, 1995), site-symmetry identification (de Groot *et al.*, 1992), and the modelling of site occupancies (Schofield *et al.*, 1993) have been described.

Waychunas and Brown (1990) found a significant polarization dependence of Fe *K*-edge X-ray absorption near-edge structure (XANES) and extended X-ray absorption fine structure (EXAFS) in gillespite single crystals. When the polarization vector lies within the plane of the FeO_4 group (perpendicular to the crystallographic *c* axis) an enhancement of two multiple scattering features occurs in the XANES region and there is a large contribution to the EXAFS from the four oxygen ligands. When the polarization vector is perpendicular to the FeO_4 square plane, a bound state transition ($1s \rightarrow 4p_z$) is enhanced, a localized continuum resonance occurs within the XANES region, and there is an 86% decrease in the contribution from the square planar oxygens to the EXAFS.

The $2p$ absorption phenomenon is analogous to the electron excitation responsible for the pre-edge features found in some of the $1s$ (*K* edge) XAS spectra. These $1s$ pre-edge features are, however, due to dipole forbidden $1s \rightarrow 3d$ transitions and are only observed when there is a mixed final state involving metal $3d$ and oxygen $2p$ orbitals. However, $2p$ absorption has a high transition probability as it involves dipole-allowed transitions of $2p$ electrons directly into the empty $3d$ states. Secondly, the core-hole lifetime broadening is up to 4 times smaller for the $2p$ transitions than for the $1s$ transitions resulting in strong and sharp multiplet lines in the $2p$ spectra. Furthermore, the advantage of studying $2p$ spectra is enhanced by the core-hole spin-orbit interaction which separates the $2p_{3/2}$ and the $2p_{1/2}$ spectral regions. We demonstrate in this paper that $2p$ XAS is an ideal probe for studying the anisotropic X-ray absorption of gillespite single-crystals.

Linear dichroism

Linear dichroism, in which the absorption of linearly polarized radiation varies between two contrasting directions, is commonly observed in anisotropic crystals with light in the visible region under the name of pleochroism. Similarly, we may use linearly polarized X-rays to measure linear dichroism. Cubic, isotropic minerals will show no variation in the absorption of linearly polarized X-rays as a function of orientation. Even if the transition metal cations are in distorted coordination sites within these isotropic minerals, the sites are orientationally disordered and hence the absorption is an average over all these sites. When the crystal and site symmetry is decreased, however, the charge distribution associated with the transition metal cation becomes distorted, resulting in anisotropic X-ray absorption. As described above, gillespite is tetragonal and the Fe^{2+} resides in square-planar geometry. Hence, the X-ray absorption will vary between extrema occurring when the polarization vector lies parallel and perpendicular to the 4-fold axis.

The use of magnetic linear dichroism for determining the magnetic moment of $3d$ transition metal and rare earth ions in (anti)ferromagnetic and ferrimagnetic materials is well established (van der Laan *et al.*, 1986; Kuiper *et al.*, 1993). Natural linear dichroism can be present in the absence of a magnetic exchange field, in which case it reflects the anisotropy of the ground state $3d$ charge distribution due to the crystal-field interaction, and hence, is of significant use in the study of mineral properties and their electronic structure. Synchrotron radiation inherently provides radiation which is linearly polarized and hence has enabled many studies of linear X-ray dichroism, predominantly at transition metal *K* edges, but more recently also in the soft X-ray region (i.e. transition metal *L* edges, oxygen *K* edges, etc.). Templeton and Templeton (1982) were the first to measure linear dichroism at the *L* edge showing that at the L_1 and L_3 edges of the uranyl ion there was a difference in edge position of 12 and 2.5 eV, respectively, depending on orientation. In the soft X-ray region many of the subsequent studies have related to the oxide superconductor phases at the Cu $2p$ edge (Flipse *et al.* 1993). van der Laan and Thole (1991) have calculated the linear dichroism in the $2p$ XAS of all $3d$ transition metal ions in octahedral crystal-fields up to 3 eV and reported a relation between the integrated intensities and the shape anisotropy.

An interesting application of linear dichroism is the possibility of obtaining direct information about the quadrupole moment of the $3d$ electrons. The $2p$ absorption measures the $3d$ hole (electron vacancy) density parallel to the polarization vector of the X-rays. Since the linear dichroism is the difference in absorption of two mutually perpendicular directions, the difference in $3d$ density between these two directions is measured. A sum rule relates the integrated intensity of the

TABLE 1. The one-hole $3d$ orbitals in O_h and D_{4h} symmetry together with the value of m and the components of the normalized quadrupole moment along z

d orbital	O_h	D_{4h}	$\lvert m \rvert$	Q_{zz}
z^2	e	a_1	0	−1
xz	t_2	e	1	−0.5
yz	t_2	e	1	−0.5
x^2-y^2	e	b_1	2	1
xy	t_2	b_2	2	1

linear dichroism to the anisotropy in the charge distribution. The latter can be expressed in terms of multipole moments. The monopole moment gives the total charge of the $3d$ electrons, and higher multipole moments give the angular distortion of this charge distribution. The atomic d orbitals can be expressed as wavefunctions Y_{lm} which have quadrupole moments: $q_{zz} = 1/2\ m^2 - 1$, where m is the azimuthal quantum number of the l shell ($-l \leqslant m \leqslant l$). The character of the d orbitals in octahedral (O_h) and square-planar (D_{4h}) symmetry together with their normalized quadrupole moment Q in the z direction are given in Table 1. The total quadrupole moment is the sum over the q_{zz}s of *all* unoccupied orbitals. A positive value of q_{zz} means that states with high values of $|m|$ are unoccupied, which makes the distribution flat in the $x-y$ plane. For a negative value the distribution is elongated along the z-axis. Thus $d(z^2)$ has a negative quadrupole moment, $d(x^2-y^2)$ and $d(xy)$ have positive quadrupole moments, and $d(xz)$ and $d(yz)$ have intermediate values (Table 1). The geometries of the electron orbitals are shown in Fig. 2. Note that we have defined the quadrupole moments for the hole distribution because XAS measures holes rather than electrons. The quadrupole moment for the electron distribution has the same value but with opposite sign, which is as expected since the total moment should be zero.

In cubic symmetry, the e orbital as well as the t_2 orbitals are degenerate which makes q_{zz} equal to zero when summed over the e or t_2 states (c.f. Table 1). Therefore, there can only be a quadrupole moment in lower than cubic symmetry, such as in square planar D_{4h}. In a D_{4h} environment the $e(O_h)$ splits into b_1 and a_1. The $b_1(x^2-y^2)$ orbital is directed towards the ligands and has the highest energy. The $a_1(z^2)$

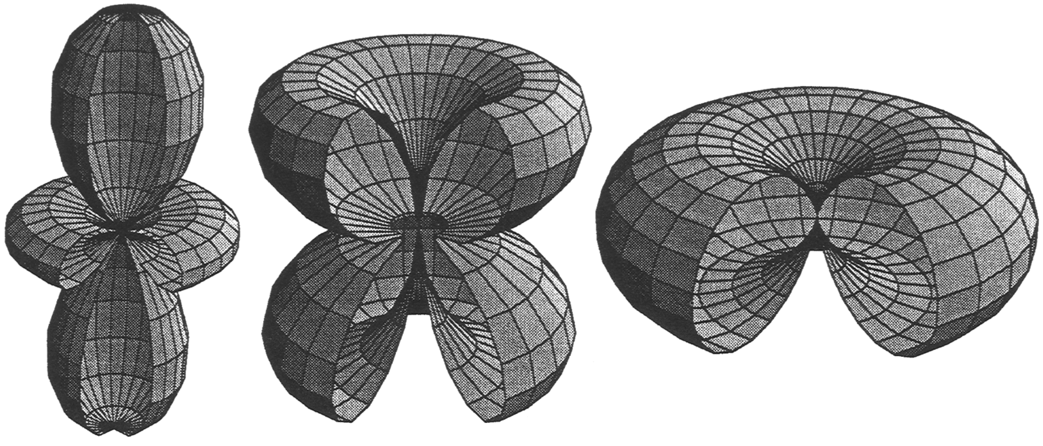

z^2
$m = 0$
$q_{zz} = -1$

$xz;\ yz$
$|m| = 1$
$q_{zz} = -0.5$

$x^2 - y^2;\ xy$
$|m| = 2$
$q_{zz} = +1$

FIG. 2. The charge distribution of the different d orbitals together with their m value and normalized quadrupole moment.

orbital is lower in energy and is usually below the $e(xz,yz)$ and $b_2(xy)$ orbitals. The distortion from the cubic symmetry results in a distinct quadrupole moment for each of the orbitals a_1, b_1, b_2 and e (Table 1).

As demonstrated by Thole and van der Laan (1993) and van der Laan (1994), the quadrupole moment is obtained by measuring the integrated linear dichroism. This can be understood from the calculated transition probabilities. From a $2p$ core level the transition probability to the sub-level m of the $3d$ level is equal to $(4 - m^2)/6$ for z-polarized light and equal to $(2 + m^2)/12$ for xy polarized light. Thus the linear dichroism defined as $I_x + I_y - 2I_z$ has an integrated intensity equal to $1/2\ m^2 - 1$ which is precisely the value of our normalized quadrupole moment. Therefore, information about the charge anisotropy can be obtained directly from the linear dichroism without having to consider the details of the XAS structure. This quadrupole moment can, in turn, be used to indicate which of the orbitals are occupied. For instance, a positive value for the integrated linear dichroism would mean that the b_1 and b_2 states are less filled than the a_1 and e orbitals (Table 1). Thus the quadrupole moment will be large for an A_1 ground state as proposed by Mackey *et al.* (1979), where the electron distribution has $d(z^2)$ character.

Experimental methods

Linearly polarized radiation in the soft X-ray region was obtained from the undulator beamline 5U.1 at the Synchrotron Radiation Source (SRS) in Daresbury (UK). The beamline is equipped with an SX700 spherical grating monochromator giving a resolution of 0.3 eV at 700 eV (Mythen *et al.*, 1992) and a beam size of about 0.5 × 0.7 mm. The samples were measured in a vacuum of 10^{-7} torr in total electron yield mode using a channeltron detector with a bias of 2.4 kV. Spectra have been normalized to the incident flux measured using a Cu grid.

A powdered spectrum was collected from a ground sample of gillespite mixed with graphite and acetone-smear-mounted onto a clean aluminium sample holder. The polarized spectra were obtained using single crystals of gillespite from the mineral collection at The Natural History Museum. Specimen numbers BM 1965,272, BM 1974,178 and BM 1980,281 have all been used in this study. Fresh cleavage fragments were attached to aluminium sample holders using either conducting glue or double sided conducting rubber stickers. The crystal dimensions were in the order of 2 × 1 mm in the xy plane and 1 mm thick.

Results

Figure 3 shows the measured spectra, for a single crystal of gillespite parallel and perpendicular to the xy-plane. These spectra are split into an L_3 ($2p_{3/2}$) edge at ~710.5 eV and an L_2 ($2p_{1/2}$) edge at ~722.5 eV, with the energy separation of ~12 eV between these two edges resulting from the core spin-orbit interaction. The L_3 ($2p_{3/2}$) edge is composed of two main peaks from the Fe^{2+} ions; the lower energy peak has a z-polarization dependence and the higher energy peak an xy-polarization dependence, where the z-axis is taken parallel to the c-direction of the crystal. A similar behaviour is also shown at the L_2 ($2p_{1/2}$) edge, but is less pronounced, as the L_2 ($2p_{1/2}$) features are intrinsically broadened due to interaction with the L_3 ($2p_{3/2}$) continuum states. The shoulders on the high energy sides of the L_3 ($2p_{3/2}$) and L_2 ($2p_{1/2}$) structures in these polarized spectra are caused by an Fe^{3+} component. This may be due to the presence of a minor impurity phase, or due to a surface layer of Fe^{3+} at the sides of the crystal that is enhanced at a glancing angle where the electron yield is increased. This structure agrees in energy

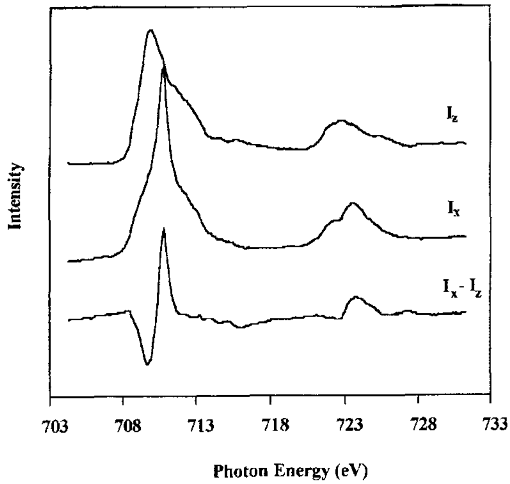

FIG. 3. Measured Fe $2p$ XAS ($L_{2,3}$) spectra for gillespite with the polarization vector parallel to z (top) and parallel to the xy-plane (middle). The linear dichroism (bottom) is displayed by the difference $I_x\ \ -I_z$.

position and shape with that of hematite (van der Laan and Kirkman, 1992). Since these Fe^{3+} features are at slightly higher energies than the Fe^{2+} peaks, the presence of this component does not affect the assignment of the polarization dependence of the double peak structure of gillespite. The natural linear dichroism is shown by the difference spectrum $I_x - I_z$ (Fig. 3). In the L_3 ($2p_{3/2}$) feature, both the high and the low energy peaks show a significant polarization dependence, whereas the low energy peak in the L_2 ($2p_{1/2}$) feature appears to show little polarization dependence.

Isotropic spectrum

In order to normalize the intensities of the polarized spectra, as well as to obtain absolute values of the quadrupole moments, it is imperative to characterize the isotropic spectrum. For cubic materials it is sufficient to measure simply a powdered specimen. However, for non-cubic phases with perfect cleavages, such as gillespite, problems of preferred orientation present a serious hinderence. Figure 4 shows the spectrum of powdered gillespite compared with a calculated isotropic spectrum (see below). It can be seen that the L_3 edge is split into two peaks of approximately equal intensity. Comparison with the calculated isotropic spectrum (Fig. 4) shows that the lower energy z-polarization component is enhanced in the powdered spectrum. Intriguingly, this is counter intuitive in that it would be expected that a layered mineral such as gillespite would lie preferentially on the cleavage plane, thus enhancing the higher energy xy-polarization component. This aspect of the powder spectrum observed is likely to be due to the stacking of the powdered gillespite platelets forming an imbricate layering structure, resulting from the acetone/gillespite/graphite slurry used in the sample preparation.

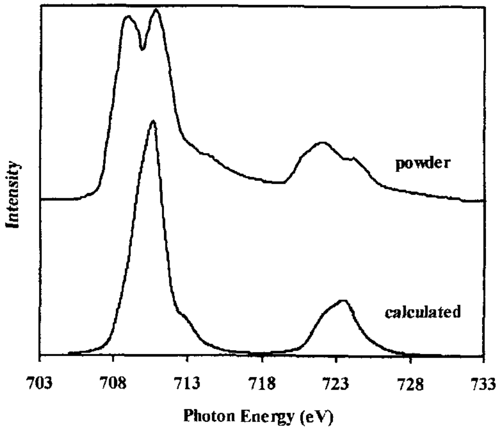

FIG. 4. The measured powdered spectrum and the expected isotropic spectrum of gillespite at 300 K as calculated from the spectra in Fig. 5.

The problem of preferential orientation can be overcome by measuring at the magic angle as described by van der Laan *et al.* (1986). For the spectral profile intensity I, measured at an angle θ between the X-ray polarization vector and the z-axis of the crystal:

$$I(\theta) = I_z \cos^2\theta + I_{xy} \sin^2\theta. \qquad (1)$$

The isotropic spectrum is then given by

$$I_{\text{iso}} = 1/3\ I_z + 2/3\ I_{xy}, \qquad (2)$$

which occurs at $\cos^2\theta = 1/3$, i.e. at the magic angle of 54.7°. Note that this trick only works well if the z and xy spectra are strongly different in shape as is the case for gillespite. Figure 5 shows a series of experimental spectra recorded at gradually increasing angles between the X-ray polarization vector and the crystallographic z-axis. When the X-ray polarization vector is in the xy-plane ($\theta = 90$) there is a minimal contribution from the z-polarization spectrum, however, as the angle moves off the xy-plane the z-polarization component (lower energy) increases.

Calculations

For the d orbitals in D_{4h} symmetry the a_1 orbital has the lowest energy. In the one-electron model, a ground state with six d electrons will therefore have a doubly occupied a_1 level and four d-holes in the remaining three levels: b_1, b_2 and e. Transitions from the $2p$ into the empty b_1 state are xyz allowed and, therefore, not polarization dependent. Transitions to the b_2 and e states are dipole forbidden. Only when the $2p$ electron is excited into an empty a_1 state would we expect a polarization dependence, since this transition is xy allowed and z forbidden. However, this transition cannot occur since in a one-electron model the a_1 state is already doubly occupied and there is no place for the excited electron. Therefore a one-electron model cannot explain the polarization dependence of the spectrum. Neither can it explain the multiplet structure, hence, we have

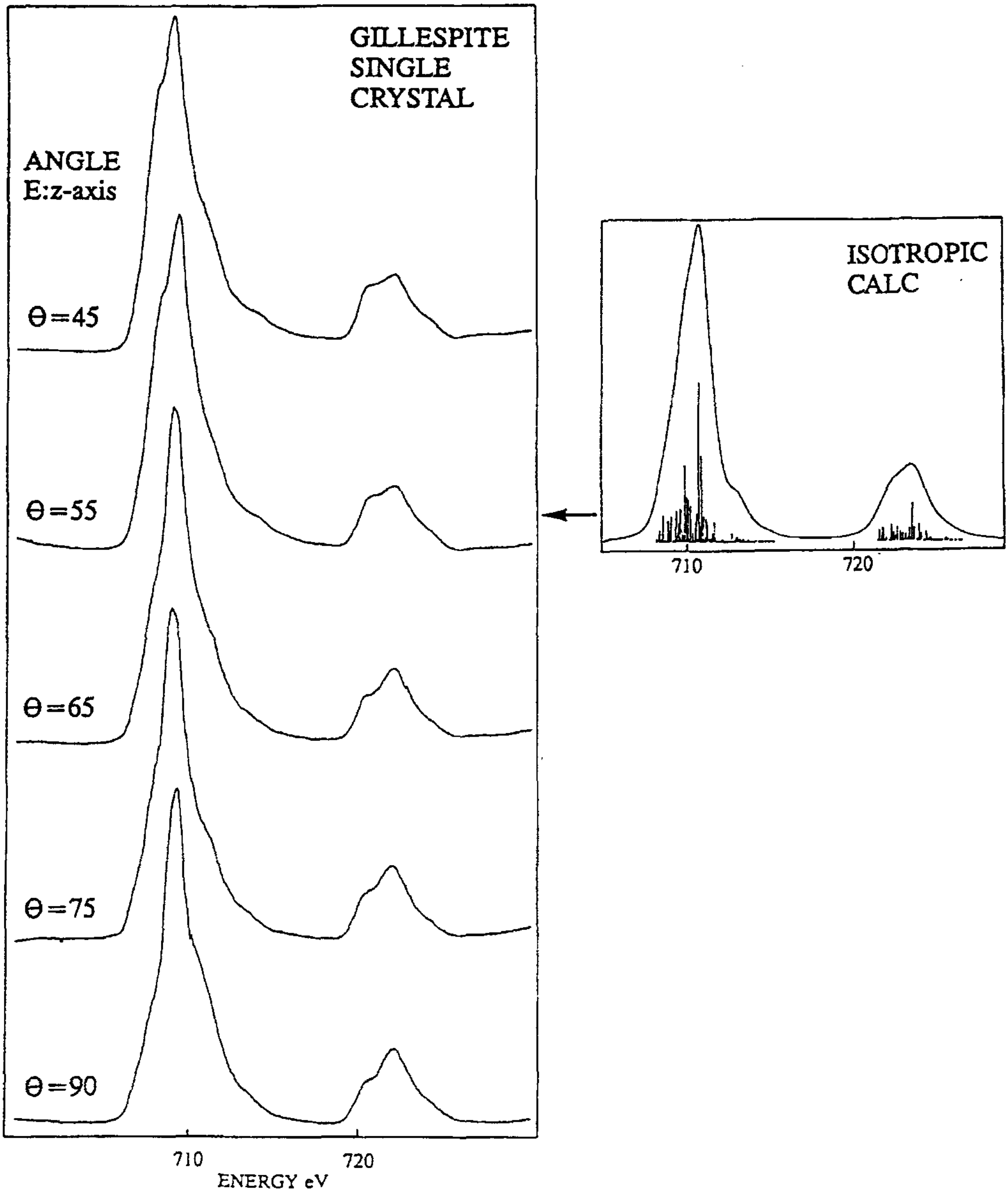

FIG. 5. A series of spectra recorded with the z-axis of the gillespite crystal at various angles θ to the X-ray polarization direction. The calculated isotropic spectrum is for T = 300 K.

to take into account the many-electron nature of our mineral. In such a description, the $2p$ absorption spectrum of a $3d$ transition metal compound is due to excitations from the crystal-field split $3d^n$ ground state configuration to $2p^5$–$3d^{n+1}$ final states, where dipole transition rules confine the subset of states that can be reached from the ground state. The final states are split by $2p$–$3d$ and $3d$–$3d$ Coulomb and exchange interaction resulting in multiplet structures 5–10 eV wide (e.g. Yamaguchi *et al.*, 1982). The $2p$ spectra of Fe d^6 ions in cubic symmetry have been given by van der Laan and Kirkman (1992). It is clear that although these spectra display a strong variation in peak shape as a function of the crystal-field parameter, $10Dq$, the double peak structure of gillespite implied by the two polarization spectra is not represented among them. Therefore, instead of cubic symmetry, we performed atomic multiplet calculations in D_{4h} symmetry.

A detailed description of these calculations is given by van der Laan *et al.* (1996) and so only a brief account is presented here. The calculated spectra which give the best fits to the measured polarization spectra are shown in Fig. 6. To account for the intra-atomic relaxation, the Coulomb parameters were reduced to 80% of their Hartree-Fock value (Lynch and Cowan, 1987) and the $2p$–$3d$ exchange to 60% (the Hartree-Fock values are listed in van der Laan and Kirkman, 1992). In principle these parameters can be included by considering the configurational interaction with the low-energy excited configurations, such as in a multi-configurational Dirac-Fock calculation. However, such an approach has little practical advantage in a solid, since there are a large number of small admixtures to the dominant configuration, and a similar result can be obtained by using reduced Slater integrals (Coulomb and exchange parameters) for a single configuration. Although the actual value of the reduction factor depends on the specific compound, the value is usually between 0.6 and 0.9. A smaller reduction factor results in a reduced multiplet width and a slightly different $L_{2,3}$ branching ratio. Apart from the crystal field, the reduction factors are the only free parameters in the calculation. We have determined the values of the reduction parameters by a best fit to the experimental spectra. The optimized crystal parameters are given in Table 2 together with those obtained from optical measurements (Mackey *et al.*, 1979). The latter are somewhat different, but in both cases the ground state is $^5A_1$ which is spin-orbit split. The spin-orbit interaction also results in a mixing of the lower levels of the ^5E excited state. The spectra are calculated for a temperature of 300 K by the inclusion of higher spin-orbit states from the ground state, weighted with the Boltzman distribution.

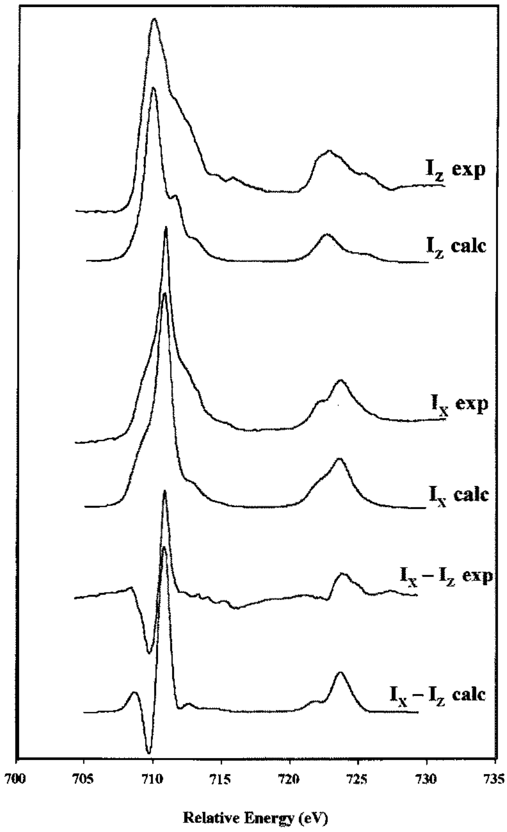

FIG. 6. Measured and calculated Fe $2p$ polarized X-ray absorption spectra for gillespite. The calculations are for Fe in D_{4h} symmetry at 300 K. Shown (from top to bottom) are spectra obtained with the X-ray polarization vector along the along the z-axis, xy-plane and the resulting difference spectrum.

The average positions of the low lying crystal-field states $^5A_1$, $^5B_2$, ^5E , $^3A_2$, relative to the spin-

TABLE 2. Crystal-field parameters (cm^{-1}) for gillespite obtained from optimization of the calculated XAS spectrum and from the optical measurements of Mackey *et al.* (1979). The esds for the crystal-field parameters are ± 5%

		XAS	Optical
Dq		1300	1150
Ds		1900	3630
Dt		1200	887
b_1	(x^2-y^2)	14000	19000
e	(xz,yz)	975	1150
b_2	(xy)	530	7500
a_1	(z^2)	0	0

orbit split ground state, are found to be 210, 750, 1200 and 8000 cm^{-1}, respectively (van der Laan *et al.*, 1996). This clearly indicates that the ground state of gillespite is $^5A_1$. Mackey *et al.* (1979) also obtained a ground state of $^5A_1$, but they suggested that the ^5E state was lower in energy than the $^5B_2$ state. The present work allows us to resolve this discrepency as the structure of the $2p$ XAS spectrum is an excellent indicator for the ground state since it is very sensitive to the symmetry of the d states. Thus, from the XAS spectra we find strong evidence for the reversal of the ^5E and the $^5B_2$ states from that proposed by Mackey *et al.* (1979) in that the orbital state b_2 is at a much lower energy than that calculated by Mackey *et al.* (1979), which results in a reversal of the energy positions of the e and b_2 states (Table 2).

$2p$ branching ratio and spin state

Thole and van der Laan (1988) showed that the branching ratio $I(2p_{3/2})/[I(2p_{3/2}) + I(2p_{1/2})]$ of the spectrum is an important diagnostic tool for distinguishing the spin state and spin-orbit interaction of the ground state. The value of the branching ratio is a measure of the electrostatic interaction between the core-hole splitting and the ground state spin-orbit splitting. What is important to us here is that high-spin states have much larger branching ratios than low-spin states. A quintet spin for Fe d^6 gives a branching ratio of ~0.75, whereas a triplet spin, which will be the ground state for $10Dq$ larger than 3 eV, has a branching ratio in the region of 0.6 to 0.65. As found for the integrated signal of the linear dichroism (see above), the branching ratio is important in that it allows us to draw general conclusions about the ground state without a detailed analysis of the spectral structure. The experimental spectra have a branching ratio of around 0.78 eV which clearly indicates that the ground state has a high spin (quintet) state. If the ground state is close to a spin transition we would expect a much lower value for the branching ratio.

The calculated isotropic spectrum at a temperature $T = 0$ K (Fig. 5) has a larger branching ratio than the isotropic spectrum at 300 K. At $T = 0$ K only the lowest spin-orbit level of the ground state is occupied. The decrease in branching ratio with increasing temperature shows that apart from the ground state level, other spin-orbit split levels also become populated within the crystal-field term. The difference in branching ratio between both polarization directions measures the correlation between the orbital and the spin moments of the same electron. The branching ratio is higher for the z-polarization than for the xy-polarization indicating that the probability of having l and s parallel is larger in the z-direction (Carra *et al.* 1993).

Since electron yield detection does not provide an absolute cross-section measurement, we have to obtain the intensities of the polarized spectra from a comparison with the isotropic spectrum, which according to Eq. (2) consists of $1/3\ I_z + 2/3\ I_{xy}$. At 0 K, where only the lowest level is occupied, the quadrupole moment is 0.93 (van der Laan *et al.*, 1996). The integrated intensity ratio, I_x / I_z at 300 K yields a quadrupole moment equal to 0.83, strengthening the argument for the determined ground state and the $d(z^2)$ character of the electron distribution.

Concluding remarks

Analysis of the branching ratio indicates that the ground state has a quintet (high) spin with hardly any mixing from low-spin states. Analysis of the detailed spectral shape shows that the ground state is $^5A_1$ with the $^5B_2$ state only about 500 cm^{-1} higher. Increased pressure along the z-axis, shown to be the most compressible axis by Hazen and Finger (1983), will distort the charge distribution and so increase the energy of the $d(z^2)$ orbital, and lower the energy of $d(xy)$. Only a small change in the crystal-field is necessary to reduce the $^5B_2$ state to the lowest energy state. These relationships are consistent with the pressure-induced colour change having a crystal-field origin, confirming the conclusion of Abu-Eid *et al.* (1973). However, we are not able to meaningfully assess the extent to which these crystal-field changes might influence the crystallographic phase transition, compared to the effects of geometric instabilities occurring within the Ba–O polyhedra or within the silicate framework.

Acknowledgements

The authors would like to acknowledge the support of the Daresbury Laboratory, and in particular the assistance of Mark Roper.

References

Abu-Eid, R.M., Mao, H.K. and Burns, R.G. (1973) Polarized absorption spectra of gillespite at high pressure. *Carnegie Institute Washington Year Book* **73**, 564–7.

Carra, P., Konig, H., Thole, B.T. and Altarelli, M. (1993) Magnetic X-ray dichroism. *Physica B Condensed Matter*, **192**, 182–90.

Cressey, G., Henderson, C.M.B. and van der Laan, G. (1993) Use of L-edge X-ray absorption spectroscopy to characterize multiple valence states of 3d transition metals; a new probe for mineralogical and geochemical research. *Phys. Chem. Mineral.*, **20**, 111–9.

de Groot, F.M.F., Figueiredo, M.O., Basto, M.J., Abbate, M., Petersen, H. and Fuggle, J.C. (1992) 2p X-ray absorption of titanium in minerals. *Phys. Chem. Mineral.*, **19**, 140–7.

Flipse, C.F.J., van der Laan, G., Thole, B.T. and Myhra, S. (1993) Polarized x-ray absorption study of $Bi_2Sr_2CuO_6$ and $Bi_2Sr_2CaCu_2O_8$. *Zeits. für Physik B*, **90**, 89–91.

Hazen, R.M. and Burnham, C.W. (1974) The crystal structures of gillespite I and II; a structure determination at high pressure. *Amer. Mineral.*, **59**, 1166–76.

Hazen, R.M. and Finger, L.W. (1983) High-temperature and high-pressure crystallographic study of the gillespite I-II phase transition. *Amer. Mineral.*, **68**, 595–603.

Henderson, C.M.B., Cressey, G. and Redfern, S.A.T. (1995) Geological applications of synchrotron radiation. *Radiation Physics and Chemistry*, **45**, 459–81.

Huggins, F.E., Mao, H.K. and Virgo, D. (1975) Mossbauer studies at high pressure using the diamond anvil cell. *Carnegie Institute Washington Year Book*, **74**, 405–10.

Huggins, F.E., Mao, H.K. and Virgo, D. (1976) Gillespite at high pressure: results of a detailed Mossbauer study. *Carnegie Institute Washington Year Book*, **75**, 756–8.

Kuiper, P., Searle, B.G., Rudolf, P., Tjeng, L.H. and Chen, C.T. (1993) X-ray magnetic dichroism of antiferromagnetic Fe_2O_3: The orientation of magnetic moments observed by Fe 2p X-ray absorption spectroscopy. *Phys. Rev. Letters*, **70**, 1549–52.

Lynch, D.W. and Cowan, R.D. (1987) Effect of hybridization on 4d-4f spectra in light lanthanides. *Physics Review, B*, **36**, 9228–33.

Mackey, D.J., McMeeking, R.F. and Hitchman, M.A. (1979) Magnetic anisotropy and electronic structure of gillespite, a mineral containing planar, four-coordinate, high-spin iron. *J. Chem. Soc. Dalton*, 299–305.

Mythen, C.S., van der Laan, G. and Padmore, H.A. (1992) The undulator beamline at the SRS Daresbury. *Review of Scientific Instrumentation*, **63**, 1313–6.

Pabst, A. (1943) Crystal structure of gillespite, $BaFeSi_4O_{10}$. *Amer. Mineral.*, **28**, 372–90.

Redfern, S.A.T., Clark, S.M. and Henderson, C.M.B. (1993) High-pressure ferroelastic phase transition in gillespite: new evidence from energy-dispersive diffraction. *Material Science Forum*, 133–6, 615–20.

Schaller, W.T. (1922) Gillespite, a new mineral. *J. Washington Academy of Science*, **12**, 7–8.

Schofield, P.F., Henderson, C.M.B., Redfern, S.A.T. and van der Laan, G. (1993) Cu) *2p* X-ray absorption spectroscopy as a probe for the site occupancy of $(Zn_xCu_{1-x})WO_4$ solid solution. *Phys. Chem. Mineral.*, **20**, 375–81.

Schofield, P.F., Henderson, C.M.B., Cressey, G. and van der Laan, G. (1995) *2p* X-ray absorption spectroscopy in the earth sciences. *J. Synchrotron Radiation*, **2**, 93–8.

Strens, R.G. (1966) Pressure-induced spin-pairing in gillespite $BaFe(II)Si_4O_{10}$. *Chemical Communications*, **21**, 777–8.

Templeton, D.H. and Templeton, L.K. (1982) X-ray dichroism and polarized anomalous scattering of the uranyl ion. *Acta Cryst.*, **A32**, 62–7.

Thole, B.T. and van der Laan, G. (1988) Branching ratio in X-ray absorption spectroscopy. *Phys. Rev., B.*, **38**, 3158–71.

Thole, B.T. and van der Laan, G. (1993) Sum rules for magnetic dichroism in rare earth 4f photoemission. *Phys. Rev. Letters*, **70**, 2499–502.

van der Laan, G. and Kirkman, I.W. (1992) The 2p absorption spectra of 3d transition metal compounds in tetrahedral and octahedral symmetry. *J. Phys.: Condensed Matter*, **4**, 4189–204.

van der Laan, G. and Thole, B.T. (1991) Strong magnetic x-ray dichroism in 2p absorption spectra of 3d transition metal ions, *Phys. Rev., B*, **43**, 13401–11.

van der Laan, G. (1994) Sum rules and fundamental spectra of magnetic x-ray dichroism in crystal field symmetry. *J. Phys. Soc. Japan*, **63**, 2393–400.

van der Laan, G., Schofield, P.F., Cressey, G. and Henderson, C.M.B. (1996) Natural linear dichroism at the Fe 2p absorption edge of gillespite. *Chem. Phys. Letters*, **252**, 272–6.

van der Laan, G., Thole, B.T. and Sawatzky, G.A. (1988) Multiplet structure in the $L_{2,3}$ X-ray absorption spectra: A fingerprint for high- and low-spin Ni^{2+} compounds. *Phys. Rev., B*, **37**, 6587–9.

van der Laan, G., Thole, B.T., Sawatzky, G.A., Goedkoop, J.B., Fuggle, J.C., Esteva, J.M., Karnatak, R.C., Remeika, J.P. and Dabkowska, H.A. (1986) Experimental proof of magnetic X-ray dichroism. *Phys. Rev., B*, **34**, 6529–31.

Wainright, J.E. (1969) Reinvestigation of the crystal structure of gillespite. *Canad. Mineral.*, **10**, 148.

Waychunas, G.A. and Brown, G.E., Jr. (1990) Polarized X-ray absorption spectroscopy of metal ions in minerals. *Phys. Chem. Mineral.*, **17**, 420–30.

Yamaguchi, T., Shibuya, S., Suga, S. and Shin, S. (1982) Inner-core excitation spectra of transition-metal compounds: II. p-d absorption spectra. *J. Phys., C: Solid State Physics*, **15**, 2641–50.

[*Manuscript received 20 August 1996: revised 2 April 1997*]